# Assignment 3

Amalia Voulgaraki - nbt146, Vasiliki Kouselini - tbm262,
Arina Zamyshevskaya - tjw488, Daria Radcenko - lzw942

15th December 2025

## 1 A bit of modelling

### Lambert's Law

Lambert's law for a generic pixel in the simplest form is denoted as follows:

$$I = \rho(s \cdot n),$$

where the pixel value $I$ is computed by scaling the dot product between the incident direction $s$ and the normal surface $n$ by the albedo $\rho$.

A self-shadow is characterized by $s \cdot n \leq 0$. To avoid a negative value for the pixel intensity, we can clamp the values, so that:

$$I = \rho \ \max(s \cdot n)$$

This assures that any negative pixel intensity is set to 0.

Lambert's law works locally. Self-shadows can be processed under Lambert's law, as these are still part of the object surface. Cast shadows are not directly on the object surface anymore, meaning that those are not accounted for in Lambert's law.

Lambert's law has a few restrictions. To apply it to an object, the object cannot be shiny, restricting it to matte surfaces. This also means it fails for translucent objects or differently textured surfaces, such as water. Lambert's law is only applicable when there is one light source, making it impossible when multiple light sources are involved. Another restriction is its locality. It cannot account for cast shadows and occlusions.

### Woodham's approach

In Woodham's approach, we have multiple different light sources. If $m$ is defined as follows:

$$m := \rho n,$$

we can subsequently obtain $\rho$ and $n$:

$$\rho = ||m||$$

$$n = \frac{m}{||m||}$$

### RANSAC

When performing RANSAC, we iteratively do least squares on the data to find inliers (useful data) and outliers (useless data) based on a predefined threshold. For $k$ light directions, we first pick a triple of light directions at random. Then, we can inverse the light matrix and obtain the surface normal vector by simple vector-matrix multiplication. We then evaluate against the threshold and check how many light directions are inliers. Once we obtain these inliers, we discard all other light directions and calculate the surface normal vector via the pseudo-inverse.

## 2 Beethoven Dataset

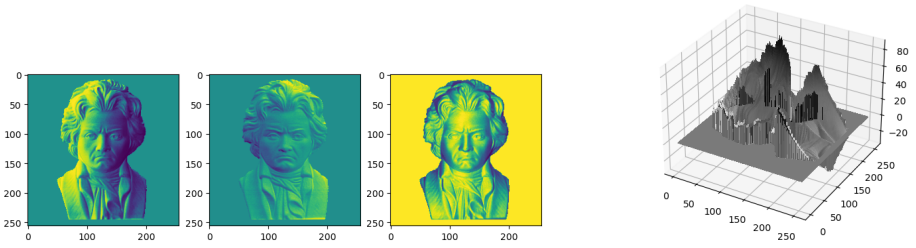

(a) Lighting Directions

(b) 3D Surface

Figure 1: Beethoven Dataset

Figure 1a shows the Beethoven data set for three different light directions. In Figure 1b, we display a 3D surface that is the result of integrating the three object views. We notice a clear reconstruction of the object outlines, while facial features seem to be more difficult to recreate.

# 3 mat_vase Dataset

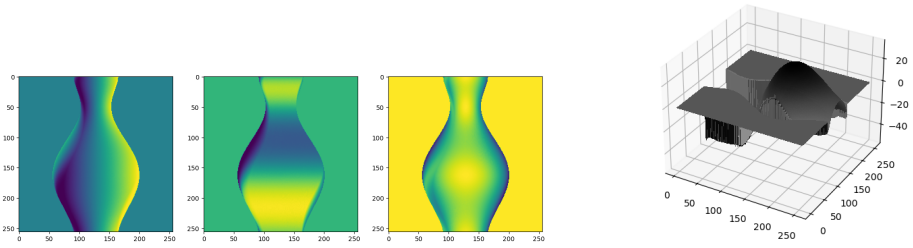

(a) Lighting Directions (b) 3D Surface

Figure 2: mat_vase Dataset

Looking at Figure 2a and 2b, we observe the same conditions as in exercise 2.

# 4 shiny_vase Dataset

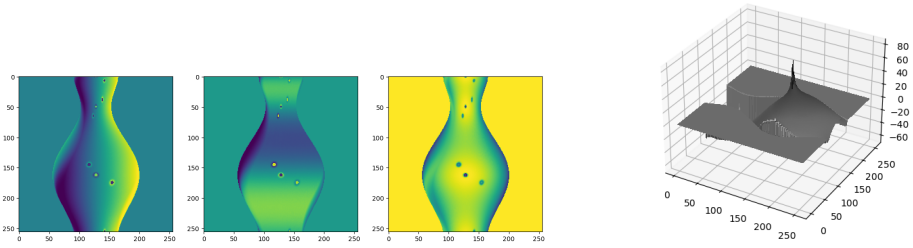

(a) Lighting Directions (b) 3D Surface

Figure 3: shiny_vase Dataset

Figure 3a displays the objects at three different light conditions. When we compute the albedo modulated normal field with the inverse of the light matrix, we observe spots on the surface and a tip protruding out of the reconstructed 3D surface (Fig. 3b). These spots are parts of the shiny surface that directly reflect into the camera. As the vase does not satisfy Lambert's law, Woodham's approach cannot perfectly deal with it.

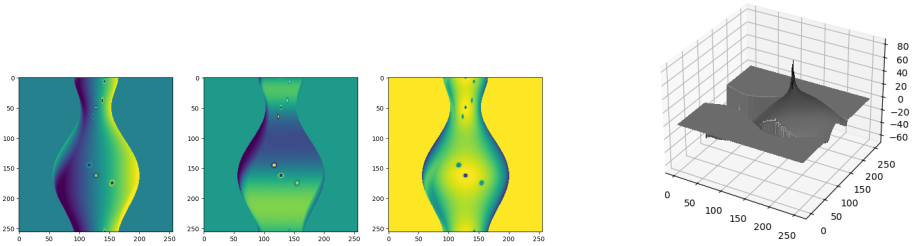

(a) Lighting Directions (b) 3D Surface

Figure 4: shiny_vase Dataset with RANSAC

Looking at Figures 4a and 4b, we notice that they seem identical to Figures 3a and 3b, which indicates that using RANSAC here does not make a difference. In computer vision, RANSAC is most useful when dealing with non-squared matrices. As we are dealing with a 3x3 matrix here, the pseudo-inverse solution reduces to the simple matrix inverse, making it effectively the same operation as Woodham's approach.

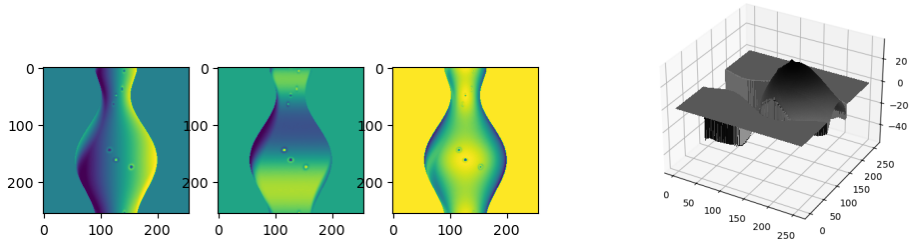

(a) Lighting Directions (b) 3D Surface

Figure 5: shiny_vase Dataset smoothed

Smoothing the normal field, we observe a slight blurring of the surface spots (Figure 5a) and a smoothing of the protruding tip (Figure 5b). The 3D surface now resembles that of a Lambertian object as displayed in Fig. 2b.

# 5 shiny_vase2 Dataset

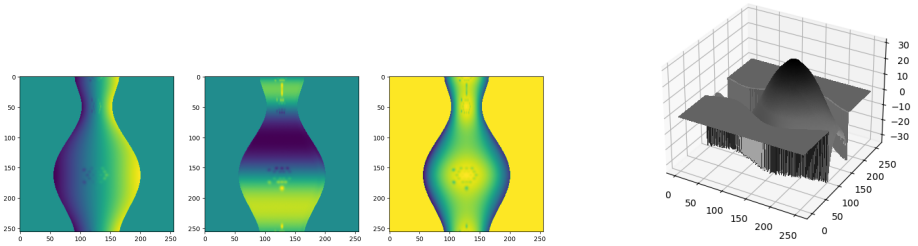

(a) Lighting Directions (b) 3D Surface

Figure 6: shiny_vase2 Dataset

Figure 6a displays the objects at three different light conditions. When we compute the albedo modulated normal field with the inverse of the light matrix, we observe spots on the surface. These spots are parts of the shiny surface that directly reflect into the camera. As the vase does not satisfy Lambert's law, Woodham's approach cannot perfectly deal with it.

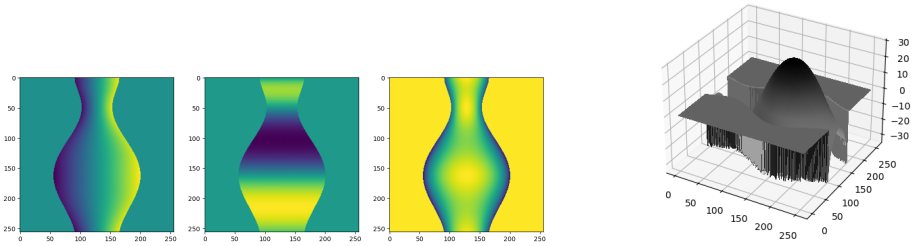

(a) Lighting Directions (b) 3D Surface

Figure 7: shiny_vase2 Dataset with RANSAC

Contrary to the shiny_vase data set, we observe a difference in the depth maps in Fig. 7a. Since we are dealing with a 22x3 matrix, we can filter out the inlier lighting directions with RANSAC and compute the pseudo-inverse. As a result, we notice a smooth object surface that resembles that of a Lambertian object.

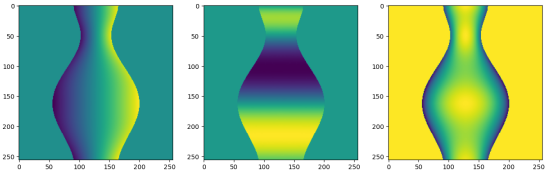

(a) Lighting Directions

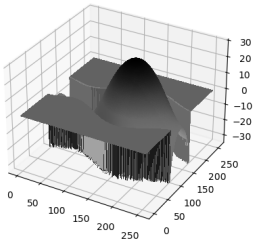

(b) 3D Surface

Figure 8: shiny_vase2 Dataset smoothed

Performing smoothing after processing the data set with RANSAC yields the same outputs as in Figure 7 as the object surface already appears smoothly.

# 6 Buddha Dataset

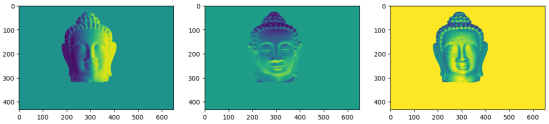

(a) Lighting Directions

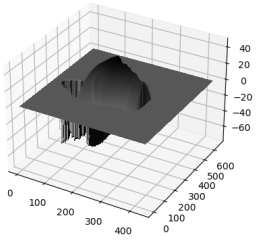

(b) 3D Surface

Figure 9: Buddha Dataset

Looking at Figure 9a and 9b, we observe the same conditions as in exercise 2.

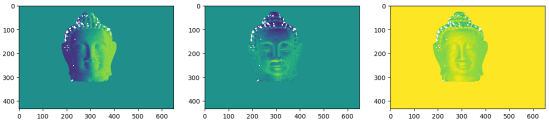

(a) Lighting Directions

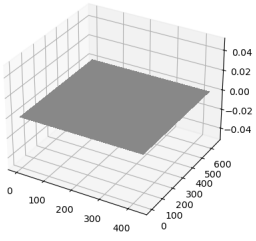

(b) 3D Surface

Figure 10: Buddha Dataset with RANSAC

In this data set, the object surface is very detailed, especially around the head region. To account for this, we use an inlier threshold of 25. After performing RANSAC, we notice white spots on Buddha's headpiece and a completely flat surface rendering in Figure 10. Additionally, we get a runtime warning when dividing by $\rho$, indicating cast shadows for $\rho = 0$. Due to the fine features on the head piece, there are a lot of spots where cast shadows may arise. On the contrary, this cannot be observed in the rest of the face, as the surface is primarily flat. Because of the missing information, the 3D surface cannot be reconstructed.

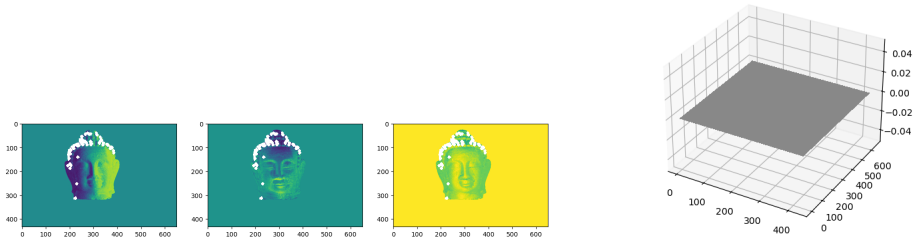

(a) Lighting Directions (b) 3D Surface

Figure 11: Buddha Dataset smoothed

When smoothing the surfaces after performing RANSAC, we observe the spots expanding in size and the same flat 3D surface (Figure 11).

# 7 face Dataset

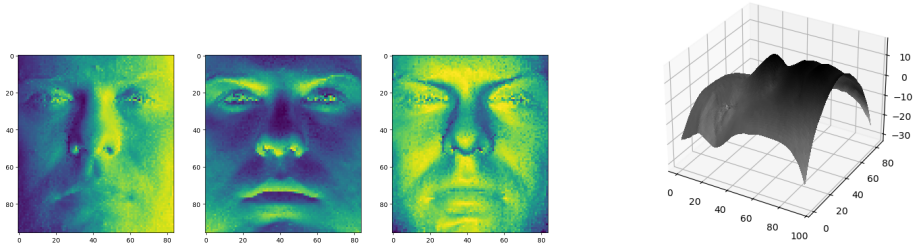

(a) Lighting Directions (b) 3D Surface

Figure 12: face Dataset with RANSAC

Looking at Figure 12a and 12b, we observe almost the same conditions as in exercise 2. Since we are working with a real data set, the images appear grainy, possibly from camera noise. Additionally, as there is no background in the images, we observe a 3D surface that consists only of the object itself.

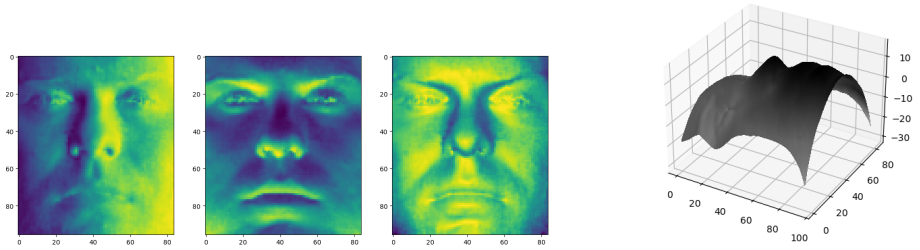

(a) Lighting Directions

(b) 3D Surface

Figure 13: face Dataset smoothed

When smoothing the images, we notice a reduction in noise at the cost of detail loss as seen in Figure 13a. While the image appears more smoothly, details, such as the eyelashes, disappear (Figure 13b).